

Thermal-radiation-induced nonequilibrium carriers in an intrinsic graphene

P.N. Romanets, F.T. Vasko,* and M.V. Strikha

Institute of Semiconductor Physics, NAS of Ukraine, Pr. Nauky 41, Kyiv, 03028, Ukraine

(Dated: November 12, 2018)

We examine an intrinsic graphene connected to the phonon thermostat at temperature T under irradiation of thermal photons with temperature T_r , other than T . The distribution of nonequilibrium electron-hole pairs was obtained for the cases of low and high concentration of carriers. For the case when the interparticle scattering is unessential, the distribution function is determined by the interplay of intraband relaxation of energy due to acoustic phonons and interband radiative transitions caused by the thermal radiation. When the Coulomb scattering dominates, then the quasi-equilibrium distribution with effective temperature and non-equilibrium concentration, determined through balance equations, is realized. Due to the effect of thermal radiation with temperature $T_r \neq T$ concentration and conductivity of carriers in graphene modify essentially. It is demonstrated, that at $T_r > T$ the negative interband absorption, caused by the inversion of carriers distribution, can occur, i.e. graphene can be unstable under thermal irradiation.

PACS numbers: 73.50.Fq, 73.63.-b, 81.05.Uv

Different kinetic phenomena caused by carriers localized near the band cross-point of graphene, including dc (magneto)transport and optical properties, have been studied intensively within recent years, see reviews [1] and last references in [2, 3]. The main attention was paid to examination of linear response of the carriers in the phonon thermostat at the temperature T . Because of the weak carrier interaction with acoustic phonons [4] different external factors can easily disturb the equilibrium of electron-hole system, and the linear response behaviour realization needs accurate control. In particular, when the sample is not isolated from external thermal radiation with temperature $T_r \neq T$, the carriers interaction with additional thermostat of thermal photons is essential. This interaction can be effective enough, because the interband transitions are determined by the velocity $v_W = 10^8$ cm/s characterizing the linear spectrum of carriers (the neutrino-like states near the band-crossing point are described by the Weyl-Wallace model [5]). Therefore graphene is very sensitive for thermal irradiation: the concentration and conductivity of carriers modify essentially (particularly, the photoconductivity induced by thermal irradiation occurs, compare with [6], where the case of the interband pumping was discussed).

In this paper, the results for the distribution of non-equilibrium carriers in the intrinsic graphene, interacting with phonon and photon thermostats with different temperatures, are presented. This distribution is obtained from the kinetic equation, taking into consideration the quasi-elastic energy relaxation due to acoustic phonons, and generation-recombination processes due to interband transitions, caused by thermal irradiation (the corresponding collision integrals were obtained in [6]). Under the high concentrations it is also necessary

to take into consideration the Coulomb scattering, which does not cause the interband transitions, see [7]. Moreover, the scattering by static disorder should be taken into account as the main mechanism of momentum relaxation [8]. In the low temperatures range, where the carrier concentration is not high, the Coulomb scattering is unessential and the distribution function differs essentially from equilibrium one due to interplay between acoustic scattering and radiative transitions. At high temperatures, when the Coulomb scattering dominates, the quasi-equilibrium distribution of carriers, with effective temperature and non-equilibrium concentration, is imposed. We also calculate the dependences of concentration and conductivity on T and T_r under the scattering by the short-range static disorder.

In the intrinsic graphene with the symmetrical c - and v -bands, and with similar scattering in these bands, the distributions of electrons and holes are identical; they are described by distribution function f_p . This function is governed by the quasi-classic kinetic equation [6]:

$$J_{BLA}(f|p) + J_{BR}(f|p) + J_{BC}(f|p) = 0. \quad (1)$$

Here the collision integrals J_{BLA} , J_{BR} and J_{BC} describe the relaxation of carriers caused by the phonon (LA) and photon (R) thermostats and the carrier-carrier scattering (C), respectively. The solutions of Eq (1) have been obtained below for the two cases: (a) low concentrations, when J_{BC} can be neglected, and (b) high concentrations, when J_{BC} imposes the quasi-equilibrium distribution with parameters determined from the equations of the balance of concentration and energy. After summation of Eq. (1) over \mathbf{p} -plane with the weights 1 and p we get these balance equations in the form [9]:

$$\frac{4}{L^2} \sum_{\mathbf{p}} J_{BR}(f_t|p) = 0, \quad (2)$$

$$\frac{4}{L^2} \sum_{\mathbf{p}} p [J_{BLA}(f_t|p) + J_{BR}(f_t|p)] = 0, \quad (3)$$

*Electronic address: ftvasko@yahoo.com

where the contribution of acoustic scattering is omitted from the equation of the concentration balance, because the interband transitions are forbidden due to the inequality $s \ll v_W$. The inter-carrier scattering does not change the concentration and energy. [7]

We start with the examination of low temperature case, when the carriers concentration is small and J_{BC} in Eq.(1) can be neglected. With the use of the collision integrals J_{BLA} and J_{BR} , presented in [6], with temperatures T and T_r correspondingly, we get the non-linear equation of the second order for the distribution function f_p :

$$\begin{aligned} & \frac{\nu_p^{\beta(qe)}}{p^2} \frac{d}{dp} \left\{ p^4 \left[\frac{df_p}{dp} + \frac{f_p(1-f_p)}{p_{BT}} \right] \right\} \\ & + \nu_p^{\beta(r)} [N_{2p/p_r}(1-2f_{pt}) - f_{pt}^2] = 0. \end{aligned} \quad (4)$$

Here we introduce the characteristic momenta $p_T = T/v_W$ and $p_r = T_r/v_W$; $N_{2p/p_r} = [\exp(2p/p_r) - 1]^{-1}$ is the Plank function. The rates of quasi-elastic relaxation at acoustic phonons, $\nu_p^{\beta(qe)} = (s/v_W)^2 v_{ac} p / \hbar$, and radiative transitions, $\nu_p^{\beta(r)} = v_r p / \hbar$, have been expressed through the sound velocity, s , and through the characteristic velocities, v_{ac} , and v_r . They separate the momentum dependence of the relaxation rates, which is proportional to the density of states. According to [8], where the temperature dependence of mobility have been examined, $v_{ac} \simeq 1.35 \cdot 10^4$ cm/s for the helium temperature (moreover $v_{ac} \propto T$), and the quasi-elastic character of scattering is determined by the small parameter s/v_W . For the case of graphene, placed between the SiO₂ substrate and cover layer, we get $v_r \simeq 41.6$ cm/s, see [6].

The boundary conditions in Eq.(4) are imposed both by the demand of the finite stream along the energy axis, when $p^4(df_p/dp + f_p)_{p \rightarrow \infty} < const$, and by the concentration balance equation (2). Because the acoustic and radiative contributions become zero under the equilibrium contributions with temperatures T and T_r correspondingly, and these two contributions trend to 1/2 at small p , we get $f_{p \rightarrow 0} = 1/2$. [10] This demand can be used as the boundary condition for the numerical solution of Eq.(4). Note, that the validity of Eq. (2) for the obtained distribution should be examined. This solution was carried out below with the use of the finite difference method and the iterations over non-linear contributions in Eq.(4), see [11].

In Fig. 1a-c the obtained distribution functions versus energy $v_W p$ for different T and T_r are presented. Due to the smallness of acoustic contribution at $p \rightarrow 0$ (see above), f_p is close to equilibrium distribution with the temperature T_r . If $T_r > T$ the distribution increases at high energies up to the range, where J_{LA} is dominant. With the further increase of $v_W p$ the distribution decreases rapidly on the scale of energies T , so that the peak of distribution is formed at the energies $\sim T_r$; this peak causes the carriers concentration of the order of equilibrium value at the temperature T_r . In this case the

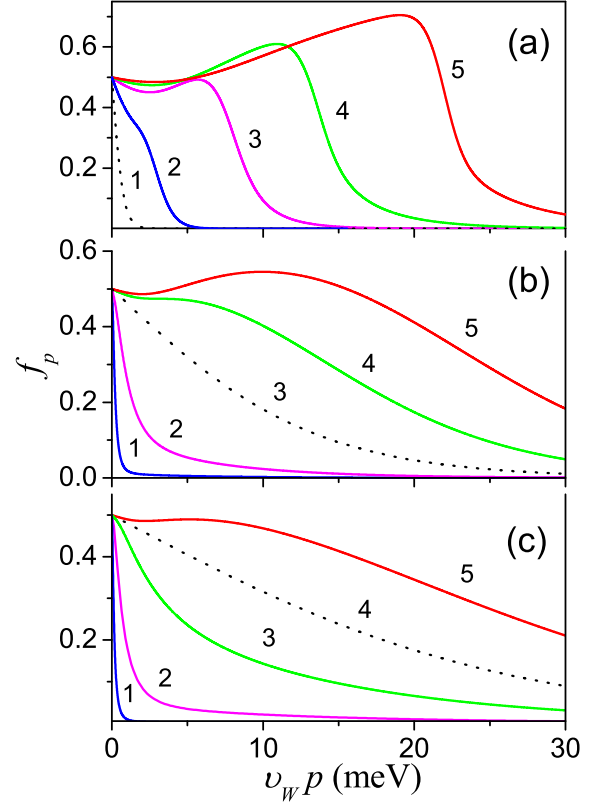


FIG. 1: (Color online) Distribution functions governed by Eq. (4) for the cases: $T=4.2$ K (a), $T=77$ K (b), and $T=150$ K (c) at $T_r=4.2$ K (1), 20 K (2), 77 K (3), 150 K (4), and 250 K (5). Dotted curves are the equilibrium thermal distributions at $T = T_r$.

condition $f_{max} > 1/2$ is realised, i.e. the inverse distribution of the carriers occupation takes place for the energies close to the maximum of distribution (see below). On the contrary, if $T_r < T$, the equilibrium contribution of the slow carriers is replaced by the rapidly decreasing part in the range of $v_W p < T$. This distribution determines the small concentration of carriers in comparison with the equilibrium value at the temperature T .

Later we shall examine the case of high temperatures (and concentrations), when the Coulomb scattering dominates, imposing the quasi-equilibrium distribution

$$\tilde{f}_p = \{ \exp[(v_W p - \mu)/T_c] + 1 \}^{-1}. \quad (5)$$

The effective temperature of carriers T_c and the chemical potential μ in this distribution are obtained from the balance equations (2) and (3). After introducing the dimensionless momentum $x = v_W p / T_c$, we get the equation of the concentration balance

$$\int_0^\infty dx x^2 \left(\frac{1 - 2\tilde{f}_x}{e^{2xT_c/T_r} - 1} - \tilde{f}_x^2 \right) = 0, \quad (6)$$

which imposes the relation between μ , and T_c/T_r , while the phonon temperature is omitted out of this equation.

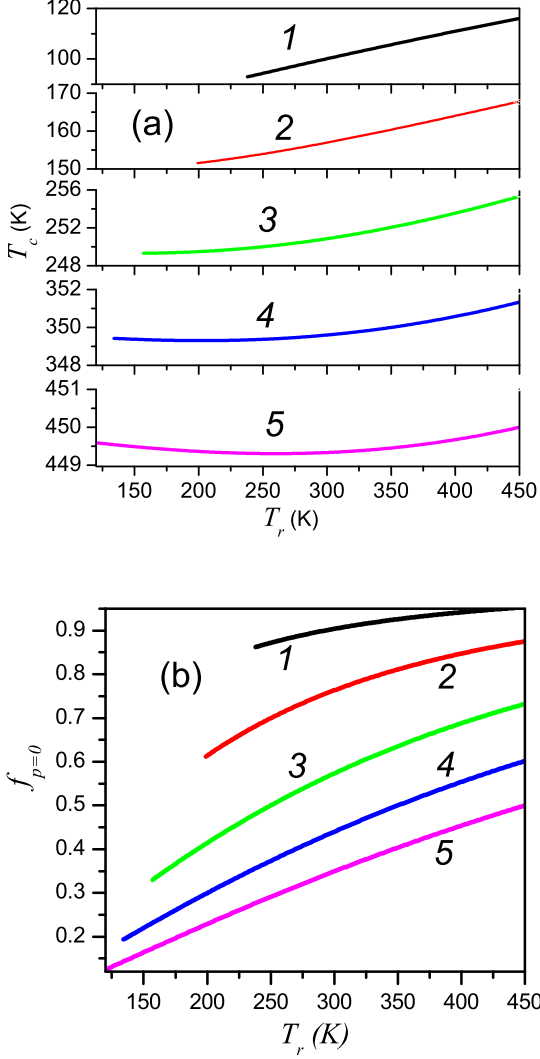


FIG. 2: (Color online) Effective temperature T_c (a) and maximal distribution $\tilde{f}_{p=0}$ (b) versus T_r for different temperatures $T = 77$ K (1), 150 K (2), 250 K (3), 350 K (4) and 450 K (5).

In these variables the equation of the energy balance can be presented as:

$$\int_0^\infty dx x^3 \left(\frac{1 - 2\tilde{f}_x}{e^{2xT_c/T_r} - 1} - \tilde{f}_x^2 \right) - \gamma \frac{T_c - T}{T} \int_0^\infty dx x^4 e^{x-\mu/T_c} \tilde{f}_x^2 = 0, \quad (7)$$

where $\gamma = (s/v_W)^2 v_{ac}/v_r \propto T$ determines the relative contribution of the phonon and photon thermostats.

The solution of the transcendental equations (6) and (7) gives the distribution (5), dependent on T and T_r , which can be characterised by the effective temperature T_c , and the maximum value of the function $\tilde{f}_{p=0} = [\exp(-\mu/T_c) + 1]^{-1}$. These values are presented in Fig.2 for the concentrations, greater than $3.5 \cdot 10^{10} \text{ cm}^{-2}$. Note, that the temperature T_c differs from T unessentially un-

der the great change of T_r , meanwhile μ and \tilde{f}_p modify essentially for the temperature range up to 450 K (the high-temperature measurements of graphene were carried out recently [12]). The essential difference of the case under examination from the low temperature solution, presented in Fig.1, is that the value $f_{p=0}$ is being fixed (and equal to 1/2), while the value $\tilde{f}_{p=0}$ decreases with the increase of T , and increases with the increase of T_r ; note, that $\tilde{f}_{p=0} = 1/2$ when $T = T_r$.

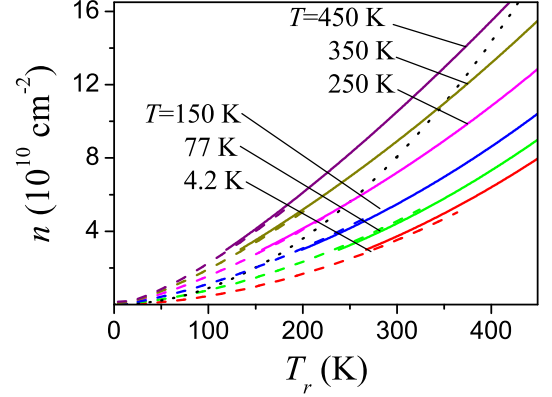


FIG. 3: (Color online) Carrier concentrations given by Eq. (8) versus temperature T_r for different T . Solutions of Eq. (4) are plotted in the range $n < 5 \cdot 10^{10} \text{ cm}^{-2}$ (dashed curves). Solutions of the balance equations (6) and (7) are plotted in the range $n > 3.5 \cdot 10^{10} \text{ cm}^{-2}$ (solid curves). The equilibrium concentration (if $T = T_r$) is shown as dotted curve.

As one can see from Figs. 1a,b or 2b, the distribution f_p or \tilde{f}_p can be greater than 1/2 in a certain energy range or at low energies. Since the inversion of electron-hole pairs occupation, the regime of the negative interband absorption can occur because the real part of dynamic conductivity is given by expression [3] $Re\sigma_\omega = (e^2/4\hbar)(1 - 2f_{p\omega})$. In the range of parameters under examination the intrinsic graphene tends to be unstable, if an additional adsorption is weak enough.

The distributions, presented in Figs. 1 and 2, are valid for the cases of low and high concentrations, correspondingly. For the calculation of non-equilibrium concentration n , dependent on T , and T_r , we use the standard expression

$$n = \frac{2}{\pi \hbar^2} \int_0^\infty dp p f_p = \frac{2}{\pi} \left(\frac{T_c}{\hbar v_W} \right)^2 \int_0^\infty dx x \tilde{f}_x, \quad (8)$$

where the right equality was written under the substitution of Eq.(5) into the standard formula. In Fig. 3 we plot n versus T and T_r for the low- and high temperature regions, when the Coulomb scattering can either be neglected, or it dominates. At $T = T_r$ these curves intersect with equilibrium concentration $\propto T^2$: because the concentration is controlled by thermal irradiation, n is smaller (or greater) then equilibrium concentration at

$T < T_r$ (or $T > T_r$). Note, that the dependences obtained from equation (4), and from the equations of balance (6), (7) correspond well in the range of intermediate concentrations, $3.5 \div 5 \cdot 10^{10} \text{ cm}^{-2}$.

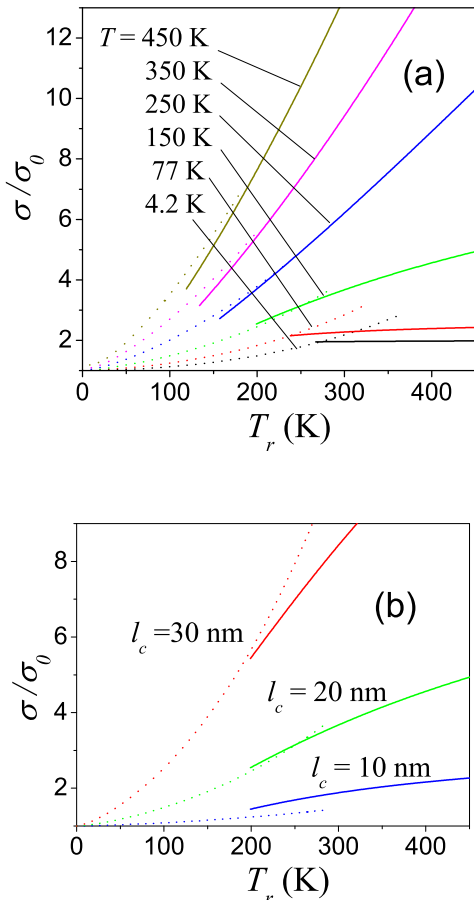


FIG. 4: (Color online) (a) Normalized conductivity, σ/σ_o , versus T_r for different T at $l_c=20$ nm. (b) The same for $T=150$ K at different correlation lengths, l_c .

The modifications of the distribution of non-equilibrium carriers in the intrinsic graphene, described above, lead to modification of conductivity, σ . For the

scattering of momenta due to static disorder with correlation length l_c we calculate the conductivity, using the formula [9]

$$\sigma = \sigma_o \left[2f_{p=0} - \frac{l_c}{\hbar} \int_0^\infty dp f_p \frac{\Psi'(pl_c/\hbar)}{\Psi(pl_c/\hbar)^2} \right], \quad (9)$$

where $\Psi(z) = \exp(-z^2)I_1(z^2)/z^2$ is written through the first order Bessel function of the imagined argument, $I_1(z)$, and σ_o is the conductivity in the case of short-range disorder scattering, when $l_c = 0$. For the case of short-range scattering, $\bar{p}l_c/\hbar \ll 1$ (\bar{p} is the characteristic momentum of non-equilibrium carriers) the conductivity is written through the low-temperature distribution: $\sigma \simeq 2\sigma_o f_{p=0}$. For the low temperature range, when $f_{p=0} = 1/2$, the conductivity depends weakly on T , and T_r . On the contrary, in the high temperature range the temperature dependences of σ on T and T_r are essential, see Fig. 4a, and Fig. 2b, where $\tilde{f}_{p=0}$ is plotted. With the increase of l_c the second term in Eq. (9) becomes essential and the thermal dependences σ/σ_o become much stronger, see Fig.4b.

Next, we list the assumptions used. The main restriction is the examination of the limit cases either of no inter-carrier collisions, or of their domination only. Despite some results correspond well in the intermediate range of concentrations and temperatures (a disagreement of σ/σ_o , versus T_r takes place at $l_c < 20$ nm only, see Fig. 4b), the accurate analysis of the intermediate range is beyond of the scope of this paper. Other assumptions, such as the models of energy spectrum, or the scattering mechanisms, as well as the simplifications of distribution function used, are rather standard for the calculations of the transport phenomena.

In closing, the consideration performed demonstrates the essential effect of thermal irradiation on the intrinsic graphene properties, therefore the transport measurements should be carried under the control of the condition $T = T_r$. Within the study of the device applications we should also consider the possible difference between the temperature of phonons and the temperature of the external thermal radiation.

-
- [1] A.H. Castro Neto, F. Guinea, N.M.R. Peres, K.S. Novoselov, and A.K. Geim, *Rev. Mod. Phys.* **XX**, (2008), arXiv:0709.1163; A.K. Geim and A.H. MacDonald, *Physics Today* **60**, 35 (2006).
[2] K. I. Bolotin, K. J. Sikes, J. Hone, H. L. Stormer, and P. Kim, arXiv:0805.1830; M. Trushin and J. Schliemann, arXiv:0802.2794.
[3] R.R. Nair, P. Blake, A.N. Grigorenko, K.S. Novoselov, T.J. Booth, T. Stauber, N.M.R. Peres, and A.K. Geim, *Science* **320**, 1308 (2008); T. Stauber, N.M.R. Peres, and A.K. Geim, arXiv:0803.1802.
[4] The optic phonons are freezed out at $T \ll 0.2$ eV,

- therefore they are unessential even for the temperatures, higher then the room one.
[5] E.M. Lifshitz, L.P. Pitaevskii, and V.B. Berestetskii, *Quantum Electrodynamics*, (Butterworth-Heinemann, Oxford 1982); P.R. Wallace, *Phys. Rev.* **71**, 622 (1947).
[6] F.T. Vasko and V. Ryzhii, *Phys. Rev. B* **77**, 195433 (2008).
[7] L. Fritz, J. Schmalian, M. Muller, and S. Sachdev, arXiv:0802.4289.
[8] F.T. Vasko and V. Ryzhii, *Phys. Rev. B* **76**, 233404 (2007).
[9] F.T. Vasko and O.E. Raichev, *Quantum Kinetic Theory*

and *Applications* (Springer, N.Y., 2005).

- [10] In order to check the condition $f_{p \rightarrow 0} = 1/2$ we have examined the transient process of the formation of the steady-state distribution, described by the equation

$$\frac{\partial f_{pt}}{\partial t} = J_{BLA}(f_t|p) + J_{BR}(f_t|p)$$

with the initial condition $t_{pt=0} = [\exp(p/p_T) + 1]^{-1}$. The

numerical computation of the Cauchy problem with the use of time iterations method gives the same steady-state distribution, as in Fig. 1.

- [11] D. Potter, *Computational Physics* (J. Wiley, London, 1973).
 [12] Q. Shao, G. Liu, D. Teweldebrhan and A.A. Balandin, *Appl. Phys. Lett.* **92**, 202108 (2008).